Ab initio quantum mechanical calculation of the reaction probability for the $Cl^- + PH_2Cl \rightarrow ClPH_2 + Cl^-$ reaction

Pooria Farahani[a],* Marcus Lundberg[a],† and Hans O. Karlsson[a‡]

[a] *Theoretical chemistry, Department of Chemistry-Ångström laboratory, Uppsala University, Box 518, SE-751 20 Uppsala, Sweden, tel: +4618-471 3260*

Abstract

The S_N2 substitution reactions at phosphorus play a key role in organic and biological processes. Quantum molecular dynamics simulations have been performed to study the prototype reaction $Cl^- + PH_2Cl \rightarrow ClPH_2 + Cl^-$, using one and two-dimensional models. A potential energy surface, showing an energy well for a transition complex, was generated using ab initio electronic structure calculations. The one-dimensional model is essentially reflection free, whereas the more realistic two-dimensional model displays involved resonance structures in the reaction probability. The reaction rate is almost two orders of magnitude smaller for the two-dimensional compared to the one-dimensional model. Energetic errors in the potential energy surface is estimated to affect the rate by only a factor of two. This shows that for these types of reactions it is more important to increase the dimensionality of the modeling than to increase the accuracy of the electronic structure calculation.

*Electronic address: Pooria.Farahani@kemi.uu.se

†Electronic address: Marcus.Lundberg@kemi.uu.se

‡Corresponding author: Hans.Karlsson@kemi.uu.se

I. INTRODUCTION

One of the most important goals of theoretical chemistry is to describe and understand the dynamics of elementary chemical reactions on the molecular level. By computing reaction rates, state-to-state probabilities and rate constants from first principles a detailed understanding of the reactions can be obtained. An important class of processes in organic chemistry for which this level of detail is of interest, is the bi-molecular nucleophilic substitution (S_N2).

The S_N2 mechanism includes the simultaneously making and breaking of single bonds, no species with double or triple bonds are involved and typically no stable intermediate is formed. In spite of having some of the simplest mechanisms in chemistry, the dynamics of the S_N2 reactions can be quite complex.[1, 2] Specially the nucleophilic substitution at carbon centers (S_N2@C) have been extensively studied, both theoretically and experimentally.[3, 4] The gas phase substitution reaction between a halide anion and a halomethane,

$$X^- + CH_3Y \rightarrow CH_3X + Y^-, \tag{1}$$

where X,Y = Cl,Br, F, I, has become an archetypal model of the S_N2 reactions.[4] The nucleophilic substitution between a halide anion and a halophosphine,

$$X^- \quad + PH_2Y \rightarrow PH_2X + Y^-, S_N2@P3, \tag{2}$$

(X,Y = Cl,Br, F, I) is valence isoelectronic with the S_N2@C, although here the central electrophilic atom is tricoordinate. In the present study, we are interested in the reaction dynamics of the gas-phase nucleophilic substitution at these phosphorus centers (S_N2@P3). The S_N2 at phosphorus centers plays a key role in organic and biological processes such as the DNA replication,[5–7] as well as in medical treatments.[8–10] In a series of papers, van Bochove et al.[11–13] used electronic structure theory to compute energy barriers and profiles for a number of different S_N2@P3 reactions. They showed that the properties of the energy profiles in terms of e.g., transition state (TS) barriers, transition complex (TC) wells and double wells, depending on the atoms involved, could be used to describe and categorize the reactions. However, these electronic structure calculations did not in detail show how the shape of the PES affects the bimolecular rate constants. In the present contribution we show how an essentially exact description of the quantum dynamics can provide significant additional understanding of the dynamics of these elementary chemical reactions.

As a prototype of the S_N2@P3 reaction we study the symmetric substitution reaction:

$$Cl^- + PH_2Cl \rightarrow ClPH_2 + Cl^-, \tag{3}$$

which is the reaction in its class with the least number of atoms. A full quantum dynamical simulation of this reaction, with $N = 5$ atoms and $N_d = 9$ degrees of freedom, is, in practice, very difficult.[4, 14, 15] It would require the handling of a 10^9 dimensional wavefunction, assuming 10 basis functions or grid points per dimension would be sufficient. Full-dimensional calculations of systems of this size have mainly been performed for reactions with a single heavy atom.[16–19] The present reaction has three heavy atoms, which leads to a significant increase in the computational cost for the quantum dynamics due to an increase in the number of basis functions or grid points, and such calculations are therefore still rare, especially for state-selected properties.[20, 21]

In addition, the $Cl^- + PH_2Cl \rightarrow ClPH_2 + Cl^-$ reaction proceeds through a transition complex well instead of a transition state barrier.[11] For direct reactions the rate is determined by the dynamics in the vicinity of the reaction barrier, and a converged rate can be computed from a simulation of the dynamics only in this region. Quantum dynamical studies of complex-forming reactions are known to be numerically more difficult due to the large phase space that are supported by the potential well, i.e., the dynamics is affected by a much larger region of the potential energy surface.[2]

To treat this complex-forming reaction with five atoms, out of which three are heavy atoms, a reduced dimensionality modeling approach has been used for the reaction dynamics. The system is modeled using the most important degrees of freedom, and using an essentially exact quantum mechanical modeling for the dynamics. The advantage with this approach is that the errors in the final result can be referred to the low dimensional modeling and the result can be systematically improved by increasing the dimensionality of the model. In the paper by van Bochove et al.[11] the modeling of reactions of the type S_N2@P3 represented in equation (2) were restricted to a one dimensional reaction path. To include dynamical effects of the reaction rates we have studied the title reaction by constructing a two-dimensional PES and computing the quantum reaction probability for both one and two-dimensional models.

II. THEORY AND INVESTIGATIONS

A. Calculating the potential energy surface

The PES was computed using second order Møller-Plesset perturbation level of theory (MP2) with the 6-31++G(d,p) basis set. To calculate the PES the two P-Cl distances were used as independent reaction coordinates. The P-Cl distances were probed from 1.0 Å to 9.0 Å with the step size of 0.05 Å. The $Cl - PH_2 - Cl$ angle was kept fixed at the transition complex geometry (168.75°) to ensure that the entire potential energy surface describes the same reaction channel, where the Cl^- approaches on the opposite side of the bound Cl atom. All the other coordinates were fully optimized at each grid point. The energy reference is taken as the sum of the energy of the two non-interacting fragments.

To test the sensitivity of the potential energy surface with respect to the electronic structure method, the geometry and relative energy of the transition complex was calculated with different computational methods. To enable a direct comparison with the study of van Bochove et al.[11] results were obtained using the density functionals OLYP and B3LYP using the 6-31++G(d,p) basis set. Calculations were also made with CCSD, using the same basis set, and with the the composite G4 method.[22] All reported energies are electronic energies and do not include zero-point or thermal corrections, and zero-point energies have therefore been subtracted from the original G4 result to enable a direct comparison with the other methods. The basis set sensitivity at the MP2 level was also tested by using basis sets from double-zeta to quadruple-zeta quality.

The Gaussian09 quantum-chemistry package was employed for the quantum chemistry calculations.[23]

B. One-dimensional model

As noted by van Bochove,[11] the 1D PES for the reaction of interest here has the form of a deep well which leads to a transition state complex.[2] It can, to first order, be described by an inverted Eckart potential,[24]

$$V = \frac{-V_0}{\cosh\left(q/\alpha\right)}, \tag{4}$$

where the depth of the well is given by V_0 and α is related to the width of the well. Here q is the reaction path coordinate. For a potential of this type, the reaction, or transmission, probability can be computed analytically as,[25, 26]

$$T(E) = \frac{\sinh^2(k\alpha/\hbar)}{\sinh^2(k\alpha/\hbar) + \cos^2(\pi z)}, \tag{5}$$

where $k = \sqrt{2\mu E}$, E is the collision energy and $z = \frac{1}{2}\sqrt{8\mu V_0\alpha^2/\hbar^2\pi^2 + 1}$. The mass of the system is given by μ and we have used that $V_0 > 0$ and $E > 0$. In equation (5) the depth of the well enters only in the cosine term. From this we can see that the accuracy in the computation of the potential well is only important at low collision energies, normally without chemical significance.

To improve the description of the one-dimensional potential over an inverted Eckhart potential, a fit to the computed minimum energy path was performed using the potential

$$V = \begin{cases} \frac{-V_0}{\cosh(q/\alpha)}, & -q_c < q < q_c \\ \sum_k \frac{c_k}{|q|^k}, & \text{otherwise.} \end{cases} \tag{6}$$

The potential as well as its derivatives were required to be analytic at the matching point q_c. Numerical calculations of the reaction probability were performed on this fitted potential and compared to the results of the analytical solution of the inverted Eckart potential.

C. Two-dimensional model

The rate constant can be computed as a Boltzmann average over the total energy E,

$$k(T) = (2\pi\hbar Q_r(T))^{-1} \int_0^\infty dE e^{-E/kT} N(E), \tag{7}$$

where Q_r is the reactant partition function and N(E) is the cumulative reaction probability (CRP). [27] The CRP can be obtained from a flux correlation function

$$N(E) = (2\pi\hbar)^{-1} \operatorname{Tr}\left[F\delta(E-H)F\delta(E-H)\right], \tag{8}$$

where F is the flux operator and H the Hamiltonian of the system. [27] The CRP gives the total reaction probability directly, without having to solve the complete state-to-state reactive scattering problem.

It was shown by Seideman and Miller[26] that the CRP (8) can be written in a more computationally tractable form as,

$$N(E) \;=\; Tr\left[P(E)\right] = \sum_n p_n(E), \tag{9}$$

where the reaction probability operator $P(E)$, with eigenvalues $p_n(E)$ between zero and one, is given by, [26]

$$P(E) \;=\; 4\Gamma_r^{1/2} G(E)^\dagger \Gamma_p G(E) \Gamma_r^{1/2}. \tag{10}$$

Here Γ_r (Γ_p) is an absorbing potential in the reactant (product) channel and $G(E) = (E + i\Gamma - H)^{-1}$ is the Green's function with $\Gamma = \Gamma_r + \Gamma_p$ [28]. The role of the absorbing potential is to maximize the absorption of all outgoing wave packets in each channel, without causing any reflections back to the reactive region of the potential energy surface.[26].

For most reactions P(E) has a very small number of non-vanishing eigenvalues, and the relevant eigenstates of P(E) can therefore be efficiently computed with iterative diagonalization using the Lanczos scheme,[28] instead of a complete diagonalization of the full matrix.

The cumulative reaction probability, which is a highly averaged quantity, converges fast and is not very sensitive to the modelling parameters. The reaction rate is therefore often the first property to be calculated for a complex systems. More information can be obtained from the state-to-state reaction probabilities $P_{n_p,n_r}(E) = |S_{n_p,n_r}(E)|^2$, where S is the scattering matrix. They give the probability for transitions between a defined vibrational and rotational quantum state of the reactant (n_r) to a certain quantum state of the product (n_p). State-to-state reaction probabilities are very sensitive to system parameters in order to converge, and require more computational effort than the total reaction rate.

The same formalism used to calculate the CRP can also be used to compute state-to-state reaction probabilities. It can be shown [29] that the S-matrix between an incoming reactant (n_r), and outgoing product (n_p) wave can be written as

$$S_{n_p,n_r}(E) \;=\; -\frac{i}{\hbar}\langle \Phi_{n_p} | \Gamma_p G(E) \Gamma_r | \Phi_{n_r} \rangle \tag{11}$$

Here the reactant/product wave function is given by

$$\Phi_n(r,R) \;=\; -\sqrt{\frac{1}{v}} e^{-ik_n R} \phi_n(r) \tag{12}$$

where ϕ_n is a channel eigenfunction and R is the coordinate for the outgoing wave.

To construct the Hamiltonian we use the symmetric coordinates $q_1 = \frac{1}{2}(R_1 + R_2)$ and $q_2 = R_1 - R_2$ where R_1 and R_2 are the two $Cl-PH_2$ bond distances. With these coordinates the Hamiltonian reads,[14]

$$H = -\frac{\hbar^2}{2M_1}\frac{\partial^2}{\partial q_1^2} - \frac{\hbar^2}{2M_2}\frac{\partial^2}{\partial q_2^2} + V(q_1, q_2) - i\Gamma(q_1, q_2), \tag{13}$$

where $M_1 = 2m_{Cl}$ and $M_2 = m_{Cl}m_{PH_2}/(4m_{Cl} + 2m_{PH_2})$. $V(q_1, q_2)$ is the calculated PES and the absorbing potentials $\Gamma(q_1, q_2)$ are quartic potentials added to induce the proper scattering boundary conditions.[26] An analytical 2-dim PES were constructed by fitting the computed points to the analytical form

$$V(R_1, R_2) = V_0 + \sum_{k,l=1}^{4} c_{kl} V_1^k V_2^l \tag{14}$$

$$V_i(R_i) = 1 - e^{-\beta(R_i - R_e)} \; i = 1, 2 \tag{15}$$

with $R_e = 1.10$ Å and $\beta = 3.25$ Å^{-1}. To perform the numerical evaluation, the system is discretized on an equidistant grid and using sincDVR for the kinetic energy operator.[28] A grid spacing of four grid points per de Broglie wave number gave a converged result. [26]

III. RESULT AND DISCUSSION

A. Potential energy well

The electronic structure calculations give an attractive potential for all P-Cl distances, with a deep well, corresponding to a symmetric Cl-PH_2-Cl complex, see Fig.1. At the MP2/6-31++G(d,p) level the depth of the well is 21.6 kcal/mol and the P-Cl distances are 2.42 Å. Due to the lone pair on phosporus, the reaction is not collinear but has a Cl-P-Cl angle of 168.7. The other methods give the same general description of the reaction, with similar geometries and relative energies of the Cl-PH_2-Cl complex, see Table 1, and the results are also in line with those presented in reference [11].

From the PH_2-Cl reactant, only minor changes in the geometry are required to reach the TS, see Fig.1. The most obvious one is an elongation of the P-Cl distance from 2.04 to 2.42 Å. There is also change in the H-P-Cl angles from 97.4 to 86.2, but this change is much smaller than for normal S_N2 reactions with carbon that require a complete inversion of the hydrogens.

Compared to the G4 benchmark value of 24.9 kcal/mol, the MP2/6-31++G(d,p) calculation used for the potential energy surface underestimates the well depth by 3.3 kcal/mol. Increasing the size of the basis set increases the barrier depth, but the converged MP2 at quadruple-zeta level instead overestimate the barrier by 2.4 kcal/mol, see the supporting information. The result could be improved by a more accurate choice of computational method, at the expense of increased computational cost. However, as will be discussed below, for the quantum dynamics simulations of this system, a deviation in the well depth of this size will not significantly change the results, and therefore the present level of theory is sufficient to describe the reaction dynamics of this system.

B. One-dimensional model

The one-dimensional potential energy profile was constructed by following the minimum energy path from reactants to products, see Fig. 2. It should be noted that even at a P-Cl distance of 9.0 Å the energy is still 3.29 kcal/mol lower than the non-interacting limit. The reason is the strong electrostatic interaction between the negative Cl^- ion and the PH_2Cl dipole. This long-distance interaction complicates the calculations as the quantum dynamics

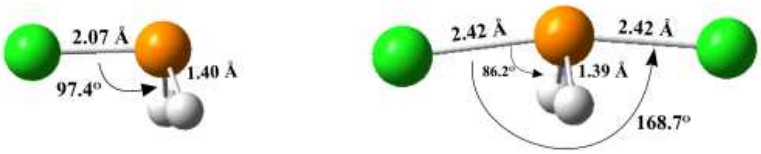

FIG. 1: Optimized reactant PH_2Cl and transition complex for the $Cl^- + PH_2Cl \rightarrow ClPH_2 + Cl^-$ reaction. Relative energies and optimized geometrical parameters at different levels of theory are given in tables 1 and S1 (supporting information).

Methods	Cl-P (1)	P-Cl (2)	P-H (3)	P-H (4)	<ClPCl	Energy well(Kcal/mol)
CCSD	2.44	2.44	1.40	1.40	168.68	20.18
MP2	2.42	2.42	1.39	1.39	168.75	21.62
DFT/B3LYP	2.42	2.42	1.42	1.42	172.00	25.46
DFT/OLYP	2.46	2.46	1.42	1.42	170.63	22.95
G4 *	2.42	2.42	1.41	1.41	169.11	24.93

TABLE 1: Bond lengths, Cl-P-Cl angles and relative energies for the Cl-PH_2-Cl complex using selected methods. All calculations are made using the 6−31++G(d,p) basis set. The exception is the G4 method where geometries are optimized using B3LYP/6-31G(2df,p), and the final energies are calculated using a composite energy approach. * Note that zero-point energies have been subtracted from the original G4 result.

are affected also by regions far away from the center of the potential energy well. Fitting an inverted Eckart potential (4), $V(q) = V(q)_{Eckart} - V_{shift}$, to the 1D PES gives $V_0 = 18.31$ kcal/mol and $\alpha = 1.08$ Ångström and $V_{shift} = 3.067$ kcal/mol, i.e. a well minimum at 21.37 kcal/mol, black line in Fig. 2.

To improve the description of the asymptotic behavior of the potential it was fitted according to equation 6 giving $V_0 = 20.81$ kcal/mol, $\alpha = 2.275$ Å and $q_c = 2.51$ Å. The resulting PES is shown as a blue line in Fig. 2.

As a first estimate the reaction probability for the one-dimensional Eckart potential can be calculated using equation 5. With the heavy mass and deep potential for the system considered here there is a unity probability for reaction, except for very low collision energies. This is a well-known situation for potentials described by equation 4, being termed reflection

free potentials.[30] For a more realistic description we also computed the reaction probability numerically for the fitted potential (6), with similar results as for the Eckart potential, i.e. no reflection for chemically relevant energies.

One question that needs to be addressed is how the accuracy of the well depth affects the transmission probability for this model. The well depth enters only in the $\cos^2(\pi z)$ term of equation 4. In Fig. 3 the transmission probability for the calculated MP2 well depth is compared to two extreme cases, namely $\cos^2(\pi z) = 1$ (maximum reflection - black dashed line) and $\cos^2(\pi z) = 1/10$ (low reflection - red dash-dotted line). For energy values higher than 0.02 kcal/mol, corresponding to a temperature of 10 K, the transmission probability is constant and equal to 1. Thus variations of the well depth within $\pm$ 3 kcal/mol, as seen in the benchmark test, will not affect the transmission probability for chemically relevant temperatures.

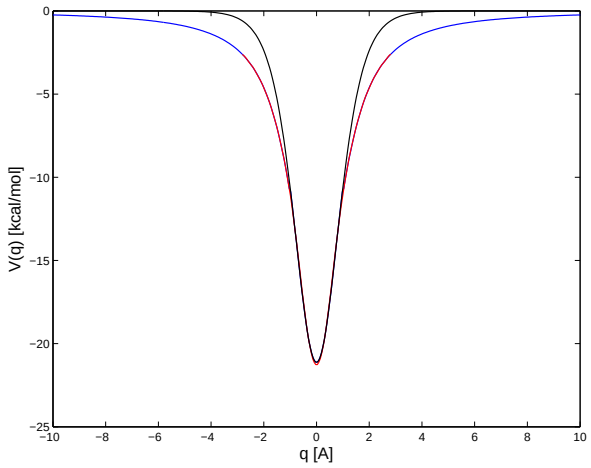

FIG. 2: The computed minimum energy path (red line) compared to an inverted Eckart potential (black line) and the combination of Eckart and polynomial potentials given by equation (6) (blue line)

The complex dynamics of this reaction cannot, however, be captured within a one-dimensional model and thus, at least, one more dimension, needs to be taken into account to describe the reaction dynamics. Looking at the changes in geometry from reactant to transition state in Fig. 1 the most obvious change is the increase in the P-Cl distances, which is why the two- dimensional model also includes movements in P-Cl distances perpendicular

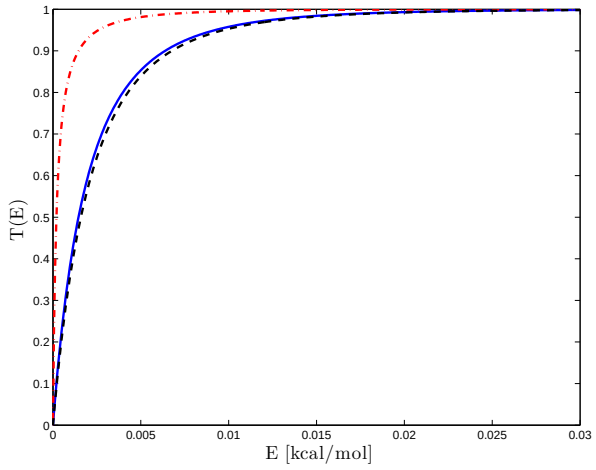

FIG. 3: Transmission probability (T(E)) *Vs* energy (E) for the calculated MP2 well depth (solid blue line) compared to the extreme case of maximum reflection $\cos^2(\pi z) = 1$ (black dashed line) and low reflection $\cos^2(\pi z) = 1/10$ (red dash-dotted line).

to the reaction coordinate. This will be discussed in the next section.

C. Two-dimensional model

The two-dimensional potential energy surface is shown in Fig.4 using the symmetric coordinates q_1 and q_2, as discussed above. The potential is symmetric with respect to coordinate q_2, the difference between the two P-Cl distances. Compared to the one-dimensional surface, the two-dimensional one includes motion perpendicular to the reaction coordinate. In the reactant this motion is the P-Cl bond stretch of the PH2Cl molecule (ν_0=552 cm^{-1}),see Fig. S1, while in the transition complex it is q_1, the symmetric Cl-P-Cl stretch (ν_0=225 cm^{-1}),see Fig. S2. More information about the molecular vibrations are given in the supporting information.

The cumulative reaction probability $N(E)$ given by equation(8) for the two-dimensional model is shown in Fig.5(a). The reaction probability is completely different from the one-dimensional model with a quite involved resonance structure in the reaction probabilities. Below 1.4 kcal/mol there is no reaction probability and this onset is due to the zero-point energy of the PH_2Cl vibration. The reaction probaility then increases rapidly around 2 kcal/mol and reaches a local maximum at 5 kcal/mol. Interestingly, between 8 and 15

kcal/mol the reaction probability is very small, with only a few resonance energies giving any appreciable probability. This is probably due to elastic scattering. Above 15 kcal/mol the probaility increases steadily, although the complicated resonance structure remains.

The involved resonance structure in the reaction probabilities indicate that there are long-lived collision trajectories. The shape of N(E) thus indicates that there are wave packets that might stay for a very long time at the transition complex geometry before going to products or back to the reactant geometry. Similar results has been observed for other PESs that support a deep well along the reaction coordinates, e.g. the $H + O_2 \rightarrow OH + H$ [31] and $Cl^- + CH_3Cl \rightarrow ClCH_3 + Cl^-$ reactions. [4]

To better understand the reaction probabilities, we have also computed the state-to-state reaction probabilities P_{n_p,n_r} from the vibrational ground state of the reactant ($n_r = 0$) to the lowest three vibrational states of the product ($n_p = 0, 1, 2$), i.e $P_{0,0}, P_{1,0}$ and $P_{2,0}$, see Fig. 5(b)-(d).

The computation of the state-to-state reaction probabilities requires a much larger grid then the cumulative reaction probability. For the state-to-state calculations a grid that extended up to 10 Å was needed for a converged result where as a grid up to 5 Å was enough for the CRP. With the heavy masses and the deep well, this is a non-trivial calculation.

In the state-to-state reaction probabilities the onset of the different vibrational channels at 1.40, 4.23 and 6.96 kcal/mol is clearly seen. $P_{0,0}$ has a complicated resonance structure, and at certain resonant energies the reaction probability is close to unity. A considerable contribution to the reaction rate is also given by $P_{1,0}$, i.e. where a reactant ground state leads to a product in the first vibrationally excited state, although the reaction probabilities are consistently lower than for the ground state to ground state reaction.

To understand how the changes in the reaction probabilities affect the reaction rate, we plot $2\pi\hbar Q_r(T)k(T)$ *versus* the inverse temperature for the computed reaction probability in Fig. 6. To illustrate the effect of over (under) estimating the depth of the potential, the rate constant is compared with results where we have increased (decreased) the depth of the well by 10%. This corresponds to a change of approximately ± 2 kcal/mol, which is in the same range as the deviation between the MP2 and the benchmark G4 result. As can be seen in Fig. 6 the rate constant changes by more than a factor of 2 in some temperature regions. This can be compared with the one-dimensional model, where the rate was independent of the well depth for energies above 0.02 kcal/mol. The rate decreases both for larger and smaller

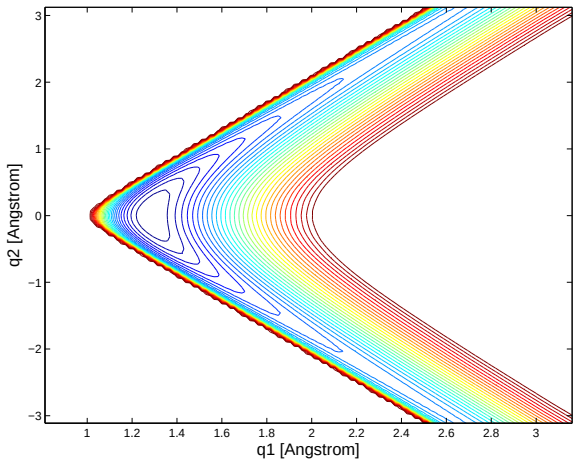

FIG. 4: The two-dimensional potential energy surface using symmetric coordinates $q_1 = \frac{1}{2}(R_1 + R_2)$ and $q_2 = R_1 - R_2$ where R_1 and R_2 are the two $Cl - PH_2$ bond distance.

.

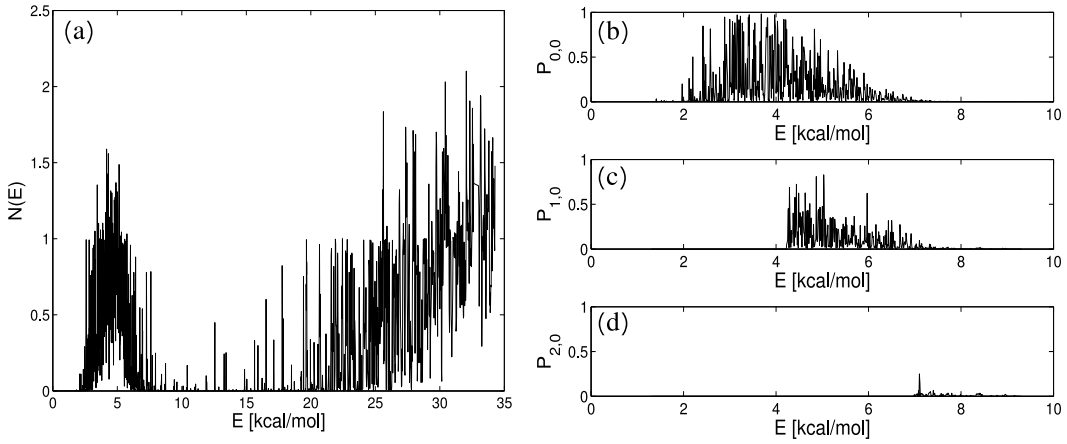

FIG. 5: (a) The cumulative reaction probability N(E) calculated using the two-dimensional potential energy surface in Fig. 4. (b) The state-to-state reaction probability $P_{0,0}$. (c) The state-to-state reaction probability $P_{1,0}$. (d) The state-to-state reaction probability $P_{2,0}$.

well depths, which shows the complicated structure of the dynamics modeling. Still, the effect of the rate constant is significantly smaller for an energy well compared to an energy barrier, where from transition state theory a similar increase or decrease in the barrier height would affect the rate by a factor of 50.

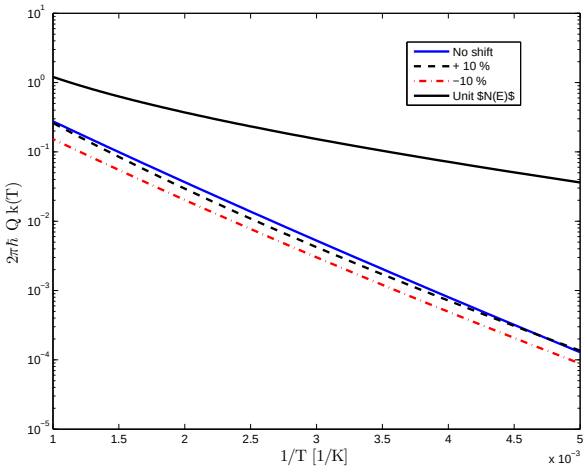

FIG. 6: Arrhenius plot of the thermal rate constant $k(T)$ times the partition function $2\pi\hbar Q_r(T)$ as a function of the inverse temperature (1/T). The sensitivity to the accuracy of the computed PES is illustrated by comparing the result with rate constants computed with a potential depth that is changed $\pm 10\%$. Included is also a comparison with the the one dimensional model, i.e. with $N(E) = 1$.

In comparison to the relatively small changes in rate with well depth, the difference in $2\pi\hbar Q_r(T)k(T)$ computed from the one and the two dimensional models is much larger, almost two orders of magnitude at room temperature. The difference is mainly due to the small reaction probabilities at lower energies, and decreases as the temperature increases because more molecules have energies between 3-5 kcal/mol where the reaction probability reaches a local maximum. The low reaction probabilities between 8-15 kcal/mol have a large effect on the reaction rate only at very high temperatures.

The results clearly show that for the present system it is more important to increase the dimensionality of the modeling than to increase the accuracy of the electronic structure calculation. A possible extension of the present model would therefore be to further increase the dimensionality of the potential energy surface [32] and in the quantum dynamics.[4] There are seven additional degrees of freedom, and the question is whether any of them would have a critical effect on the calculated reaction rates. Out of the nine vibrational frequencies of the transition complex, see the Supporting information, the antisymmetric and symmetric Cl-P-Cl stretches are already included in the two-dimensional model.

Comparing the geometry differences between the reactant and transition states, see Fig. 1, the changes in P-Cl distance and H-P-H angle are small. The most obvious change is in the Cl-P-H angle that decreases from 97.4 to 86.2 degrees, which in the transition complex corresponds to a PH_2 rocking mode with a frequency of 923 cm $^{-1}$, see Fig S1. In the related S_N2@C, this corresponds to the umbrella mode of CH_3 inversion for which excitations to higher vibrational states accelerates the reaction rate as they facilitate the geometrical distortion required to reach the transition state. The effect is not as significant for excitations of the reactant P-Cl stretch.[33, 34]

In the present S_N2@P3 reaction, the change of this coordinate is much smaller, and the corresponding effect can therefore also be expected to be smaller. The only reaction coordinate that was explicitly frozen in the modeling of the potential energy surface was the Cl-P-Cl angle, and a possible extension of the model would be to allow this angle to vary. In the S_N2@C the three hydrogen atoms impose a strong sterical constrain on the approach of the chloride,[35] while the present reaction center has one hydrogen less, and can therefore accept a much wider range of angles. The P-H distances changes by only 0.01 Å and the symmetric and asymmetric P-H bond stretch can therefore at first approximation be treated as spectators. In S_N2@C the high-frequency C-H stretch can still have a non-negligible effect on the reaction probailities at low temperature when coupled to other reaction coordinates, e.g., the CH_3 inversion in S_N2@C, in a higher dimensionality model.[36] For the present reaction the absolute effect of the PH_2 rocking mode is expected to be smaller than for CH_3 inversion, and the effects of secondary couplings should therefore also be smaller.

In this work we have considered a gas-phase reaction. If the reaction would instead take place in solvent, two separate solvent effects could be imagined. First, the dielectric effects would significantly stabilize the reactants relative to the transition complex, and the depth of the potential well would decrease. For the one-dimensional model, this would not have any noticeable effect on the reaction rate, but in the two dimensional model the effect is uncertain as the relation between well depth and reaction rate is complex, see Fig. 6. Another possible effect could come from collisions with solvent molecules that lead to energy transfer. In the two-dimensional mode, the long-lived trajectories increase the chance of energy loss to the solvent, which would cause molecules to stay even longer in the potential well. Including an energy loss mechanism would therefore further enhance the difference in reaction rate between the one and the two-dimensional model.

IV. CONCLUSION

Quantum mechanical reaction probabilities were computed for the $Cl^- + PH_2Cl \rightarrow ClPH_2 + Cl^-$ reaction using one and two-dimensional modeling, based on novel *ab initio* potential energy surfaces. The one-dimensional model is reflection free for all chemically relevant collision energies whereas the two-dimensional model displays involved resonance structures in the reaction probability. This clearly shows that a one-dimensional reaction path modeling of the reaction is not sufficient to describe the involved reactions dynamics, supporting long lived resonance states. One advantage of using a reduced dimensionality model, as has been done in this study, is that the model can be systematically improved by including more degrees of freedom. For this system next step would be to include variations of the the $Cl - PH_2 - Cl$ angle to see how the reaction probabilities are affected.

V. ASSOCIATED CONTENT

Supporting Information

Reactant and transition complex normal modes. Geometries and relative energies at the MP2 level of theory using different basis sets.

VI. ACKNOWLEDGMENTS

We would like to thank Nessima Salhi and Daniel Roca-Sanjuán for helpful comments and discussion. PF acknowledges financial support from Behrouz Nik Ind. ML acknowledges financial support from the Marcus and Amalia Wallenberg foundation. The computations were performed on resources provided by SNIC through Uppsala Multidisciplinary Center for Advanced Computational Science (UPPMAX) under Project p2011004.

References

[1] S.C. Ingold. Structure and mechanism in organic chemistry. Cornell University Press, 1969.

[2] H. Guo. *Int. Rev. Phys. Chem.*, 31 (2012) 1.

[3] J.K. Laerdahl, E. Uggerud. *Int. J. Mass Spectrom.*, 214 (2002) 277.

[4] S. Schmatz. *ChemPhysChem*, 5 (2004) 600.

[5] E.T. Kool. *Annu. Rev. Biophys. Biomol. Struct.*, 30 (2001) 1.

[6] M.R. Sawaya, R. Prasad, S.H. Wilson, J. Kraut, H. Pelletier. *Biochem.*, 36 (1997) 11205.

[7] W.A. Beard, S.H. Wilson. *Chem. Rev*, 106 (2006) C382.

[8] X. Cao, C. Liu, Y. Liu. *J. Theor. Comput. Chem.*, 11 (2012) 573.

[9] P. Dallas, V.K. Sharma, R. Zboril. *J. Theor. Comput. Chem.*, 166 (2011) 119.

[10] I. Un, H. Ibisoglu, A. Kilic, S.S. Sahin-Un, F. Yuksel. *Inorg. Chim. Acta*, 387 (2012) 226.

[11] M.A. van Bochove, M. Swart, F.M. Bickelhaupt. *J. Am. Chem. Soc.*, 128 (2006) 10738.

[12] M.A. van Bochove, M. Swart, F.M. Bickelhaupt. *ChemPhysChem*, 8 (2007) 2452.

[13] M.A. van Bochove, M. Swart, F.M. Bickelhaupt. *Phys. Chem. Chem. Phys.*, 11 (2009) 259.

[14] D.J. Tannor. Introduction to quantum mechanics. University Science Books, 2007.

[15] U. Manthe. *J. Theor. Comput. Chem.*, 1 (2002) 153.

[16] F. Huarte-Larranaga, U. Manthe. *J. Chem. Phys.*, 113 (2000) 5115.

[17] T. Wu, H.J. Werner, U. Manthe. *Science*, 306 (2004) 2227.

[18] G. Schiffel, U. Manthe. *J. Chem. Phys.*, 132 (2010) 191101.

[19] G. Schiffel, U. Manthe. *J. Chem. Phys.*, 133 (2010) 174124.

[20] F. Huarte-Larranaga, U. Manthe. *J. Chem. Phys.*, 117 (2002) 4635.

[21] S. Liu, X. Xu, D.H. Zhang. *J. Chem. Phys.*, 135 (2011) 141108.

[22] L.A. Curtiss, P.C. Redfern, K. Raghavachari. *J. Chem. Phys.*, 126 (2007) 084108.

[23] M.J. Frisch, G.W. Trucks, H.B. Schlegel, G.E. Scuseria, M.A. Robb, J.R. Cheeseman, G. Scalmani, V. Barone, B. Mennucci, G.A. Petersson, H. Nakatsuji, M. Caricato, X. Li, H. P. Hratchian, A. F. Izmaylov, J. Bloino, G. Zheng, J. L. Sonnenberg, M. Hada, M. Ehara, K. Toyota, R. Fukuda, J. Hasegawa, M. Ishida, T. Nakajima, Y. Honda, O. Kitao, H. Nakai, T. Vreven, J. A. Montgomery, J. E. Peralta, F. Ogliaro, M. Bearpark, J. J. Heyd, E. Brothers, K. N. Kudin, V. N. Staroverov, R. Kobayashi, J. Normand, K. Raghavachari, A. Rendell, J. C. Burant, S. S. Iyengar, J. Tomasi, M. Cossi, N. Rega, J. M. Millam, M. Klene, J. E. Knox, J. B. Cross, V. Bakken, C. Adamo, J. Jaramillo, R. Gomperts, R. E. Stratmann, O. Yazyev, A. J. Austin, R. Cammi, C. Pomelli, J. W. Ochterski, R. L. Martin, K. Morokuma, V. G. Zakrzewski, G. A. Voth, P. Salvador, J. J. Dannenberg, S. Dapprich, A. D. Daniels, Ö. Farkas, J. B. Foresman, J. V. Ortiz, J. Cioslowski, D. J. Fox. *Inc.: Wallingford, CT*, 2009.

[24] C. Eckart. *Phys. Rev. A*, 35 (1930) 1303.

[25] L.D. Landau, E.M. Lifshitz, J.B. Sykes, J.S. Bell, M.E. Rose. *Phys. Today*, 11 (1958) 56.

[26] T. Seideman, W.H. Miller. *J. Chem. Phys.*, 96 (1992) 4412.

[27] W.H. Miller, S.D. Schwartz, J.W. Tromp. *J. Chem. Phys.*, 79 (1983) 4889.

[28] U. Manthe, T. Seideman, W.H. Miller. *J. Chem. Phys.*, 99 (1993) 10078.

[29] W.H. Thompson, W.H. Miller. *Chem. Phys. Lett.*, 206 (1993) 123.

[30] N. Kiriushcheva, S. Kuzmin. *Am. J. Phys.*, 66 (1998) 867.

[31] C. Leforestier, W.H. Miller. *J. Chem. Phys.*, 100 (1994) 733.

[32] X. Zhang, B.J. Braams, J.M. Bowman. *J. Chem. Phys.*, 124 (2006) 021104.

[33] D.C. Clary, J. Palma. *J. Chem. Phys.*, 106 (2997) 575.

[34] H.G. Yu, G. Nyman. *Chem. Phys. Lett.*, 312 (1999) 585.

[35] S. Schmatz, D.C. Clary. *J. Chem. Phys.*, 109 (1998) 8200.

[36] C. Hennig, S. Schmatz. *J. Chem. Phys.*, 121 (2004) 220.